

Case Report

Diffusion-Weighted Magnetic Resonance Imaging and Magnetic Resonance Spectroscopy Features of Abdominal Viscera in a Patient with Gaucher's Disease

Tugce Ozlem KALAYCI, Gulnur ERDEM, Ramazan KUTLU,
Aysegül KAHRAMAN, Alpay ALKAN

Submitted: 26 Sep 2013
Accepted: 17 Feb 2013

Inonu University, Medical Faculty, Department of Radiology, 44100,
Malatya, Turkey

Abstract

A 46-year-old woman with Gaucher's disease (GD) consulted our clinic for abdominopelvic magnetic resonance imaging (MRI), as physical examination had revealed hepatosplenomegaly. Upper abdominal MRI showed massive hepatosplenomegaly and innumerable hypointense splenic nodules on T1-weighted images. Diffusion-weighted MRI (DW-MRI) and magnetic resonance spectroscopy (MRS) were performed to liver parenchyma and splenic nodules. MRS revealed lactate, lipid, acetate, and alanine peaks in splenic nodules, and choline, creatine, lipid, myo-inositol-glycine, and lactate peaks in the liver parenchyma. The DW-MRI showed diffusion restriction in splenic nodules. It was concluded that MRI is a reliable method for the diagnosis and follow up of GD. Coupling DW-MRI and MRS allows quantitative evaluation, thereby increasing the efficacy of the method. This is the first report in the literature presenting advanced abdominal MRI findings in GD.

Keywords: *diffusion magnetic resonance imaging, Gaucher disease, magnetic resonance spectroscopy*

Introduction

Gaucher's disease (GD) is a lysosomal storage disease (LSD) which develops because of deficiency in the enzyme β -glucocerebrosidase, and it shows autosomal recessive inheritance. It mainly results in problems in the skeletal system due to hepatosplenomegaly and bone marrow infiltration caused by glycosphingolipid storage in monocyte-macrophage systemic cells (1). With the development of enzyme replacement treatment, reliable imaging strategies were needed to trace the patients' reaction to treatment. Thanks to its high-resolution multiplanar imaging capacity, magnetic resonance imaging (MRI) has become the most effective modality to meet this need (2). Some authors have reported results from diffusion-weighted MRI (DW-MRI) and magnetic resonance spectroscopy (MRS) on GD in different regions of body, such as bone marrow and the central nervous system (CNS) (3,4). In this study, we present conventional MRI findings from the affected spleen and liver of a patient with GD, followed up for 18 years, as well as the findings of DW-MRI and MRS.

Case Report

A 46-year-old woman with GD consulted our clinic for abdominopelvic MRI, as her physical examination had revealed hepatosplenomegaly. DW-MRI and MRS were performed to liver parenchyma and splenic nodules.

MRI was performed using a 1.5-T system (Gyrosan Intera; Philips, Best, Netherlands). T1-weighted images (WI) (time repetition [TR]/ time echo [TE], 10/4.6) and T2-WI (1600/100) with 5 mm thick sections were obtained in the axial and coronal planes. DW-MRIs were acquired in the axial plane using single-shot echo-planar spin echo sequences obtained when the subject was breathing normally. The parameters of the DW-MRI were as follows: TR: 4393 ms; TE: 81 ms; field of view (FOV): 350 mm, number of excitations: 2; matrix size: 128 \times 256; section thickness: 5 mm; slice number: 72; intersection gap: 1 mm; and acquisition time (three gradients): 96 s. Single voxel MR spectroscopic (SVS) datasets were acquired using point-resolved spectroscopy (PRESS) ^1H MR spectra with a short (31 ms) and long (136 ms) TE.

Upper abdominal MRI showed massive hepatosplenomegaly where the cephalocaudal diameters of the liver and spleen were found to be 23 cm and 32 cm, respectively. In addition, innumerable hypointense splenic nodules were observed on T1-WI. Splenic nodules varied in signal intensity. Many of the nodules were hypointense, while some were hyperintense or of mixed intensity on T2-WI (Figure 1). While some nodules showed peripheral contrasting after intravenous contrast material, others showed heterogeneous internal enhancement. The nodules ranged in size from a few millimetres to 4 cm. Lower abdominal MRI showed a comprehensive increase in signal in pelvic bones, compatible to bone marrow infiltration with fat suppression.

MRS revealed lactate, lipid, acetate, and alanine peaks in splenic nodules with TE 136, and choline, creatine, lipid, myo-inositol-glycine, and lactate peaks in the liver parenchyma with TE 31 ms (Figure 2). The DW-MRI showed diffusion restriction in the splenic nodules. While the nodules had apparent diffusion coefficient (ADC) parameters in the range of $215\text{--}770 \times 10^{-6} \text{mm}^2/\text{s}$, the mean ADC value for normal spleen parenchyma was measured as $1157 \times 10^{-6} \text{mm}^2/\text{s}$. The mean ADC value for liver was found to be $919 \times 10^{-6} \text{mm}^2/\text{s}$.

Discussion

In 1882, Philippe Charles Ernest Gaucher described a 32-year-old woman with massive splenomegaly and unusually large cells in the spleen, which he called a 'primary epithelioma of the spleen'. This disease was the first LSD described and has become a prototype for the

clinical description and phenotypic variability of more than 50 LSDs (1). GD is characterised by anaemia and a coagulation disorder caused by growths in liver and spleen and the infiltration of Gaucher's cells into the bone marrow (2,5). The degree of splenomegaly is always higher than that of hepatomegaly (5). Similarly, in our case involving hepatosplenomegaly, the cephalocaudal diameter of the liver was higher than that of the spleen. Splenic nodules are common, and are seen in 30% of patients with GD; however, for the distinctive diagnosis of Gaucher patients with splenic nodules, malign splenic masses such as lymphoma and leukaemia should be considered first (6). The size of nodules varies from 5 to 60 mm in maximal diameter. Hepatosplenomegaly and many splenic nodules can be imaged on ultrasound (US), computed tomography (CT) and MRI. Nodules can be seen as well-circumscribed round masses with unstable signal intensity on MRI. While most nodules are isointense on T1-WI or hypointense on T2-WI, some nodules can have high signal intensity on T1-WI or T2-WI. In addition, some nodules can be seen with mixed intensity, which appear to have a target configuration with a hypointense centre and hyperintense rim on T2-WI (5,6). In our case, splenic nodules were varied in signal intensity, but most were hypointense on T1-WI.

Abnormal signal intensity can be seen in 20% of GD patients' livers on MRI. High signal areas on T2-WI are compatible with inflammation, fibrosis and/or ischaemia and relative ischaemia areas caused by the infiltration of hepatic sinusoids with Gaucher's cells (5). No abnormal signal areas were observed in the liver of the case presented in this study.

Radiographical findings on the skeletal

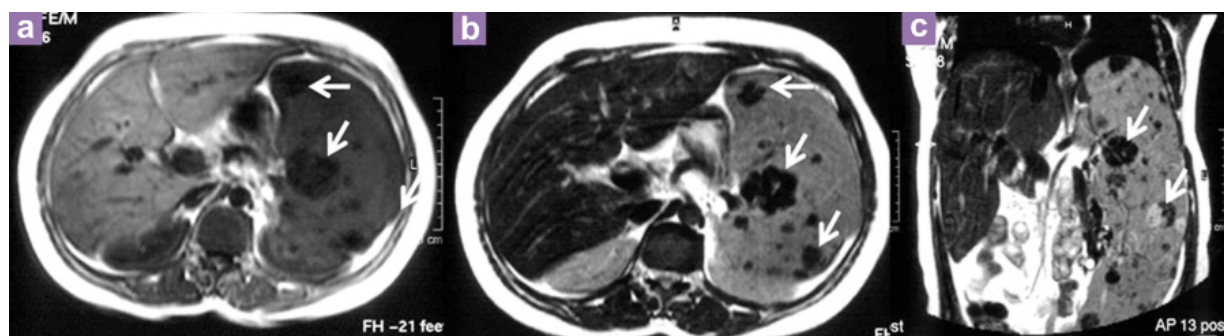


Figure 1: Axial (a,b) and coronal (c) abdominopelvic magnetic resonance imaging of a 46-year-old woman with Gaucher's disease and hepatosplenomegaly. Many splenic nodules (white arrows) exhibit low signal intensity on axial T1-WI, and most have low signal intensity on axial T2-WI and coronal T2-WI.

system and CT and US findings on the liver and spleen for patients with GD were defined. In addition, MRI findings related to bone and abdominal viscera were reported (2,5). Conventional MRI is a useful technique in GD, but the main drawback of conventional MRI is that it is not quantitative. DW-MRI and MRS give quantitative information for evaluating the liver and spleen in patients with GD, but they are not widely available.

DW-MRI is a non-invasive imaging method enabling the quantitative measurement of diffusion activity in water molecules in tissue. While diffusion restriction increases in tissues with higher signal intensity, it decreases in tissues with lower signal intensity because of large extracellular distance or when the integrity of the cell membrane is disrupted (7,8). ADC values of CNS and bone marrow in GD have been reported in literature. Abdel Razek et al. performed a study which included 20 infants and children with GD and 20 age- and sex-matched controls. They found a significant difference in the ADC values of vertebral bone marrow between children with GD and controls (3). In another study, the researchers reported significantly lower ADC value of the cortical white matter, corticospinal tract, cerebellum, medulla and midbrain between

patients with GD and healthy volunteers (4).

In the present case, DW-MRI revealed ADC values in the range of $215\text{--}770 \times 10^{-6} \text{ mm}^2/\text{s}$ in splenic nodules, and a mean ADC value of $1157 \times 10^{-6} \text{ mm}^2/\text{s}$ in normal spleen parenchyma. We contend that the diffusion restriction observed in splenic nodules is caused by increased Gaucher's cell proliferation.

We measured the mean ADC value of the liver as $919 \times 10^{-6} \text{ mm}^2/\text{s}$. Kılıçkesmez et al. (7) reported ADC values of the normal abdominal viscera and found that the mean ADC values of the normal liver were varied in the range of $1340\text{--}1770 \times 10^{-6} \text{ mm}^2/\text{s}$ according to the segment. This is compatible with liver diffusion restriction in GD when compared to the value in the present case.

MRS is a functional imaging method which gives information about the biochemical structure and metabolisms of tissues. Using this method, levels of various chemical metabolites can be measured. Results for MRS of the brain in patients with GD have been reported in the literature. Proton MRS of white matter in 21 children with acute and chronic forms of neuronopathic GD was performed and the researchers found a significant difference in choline/creatine between patients and the control group. They

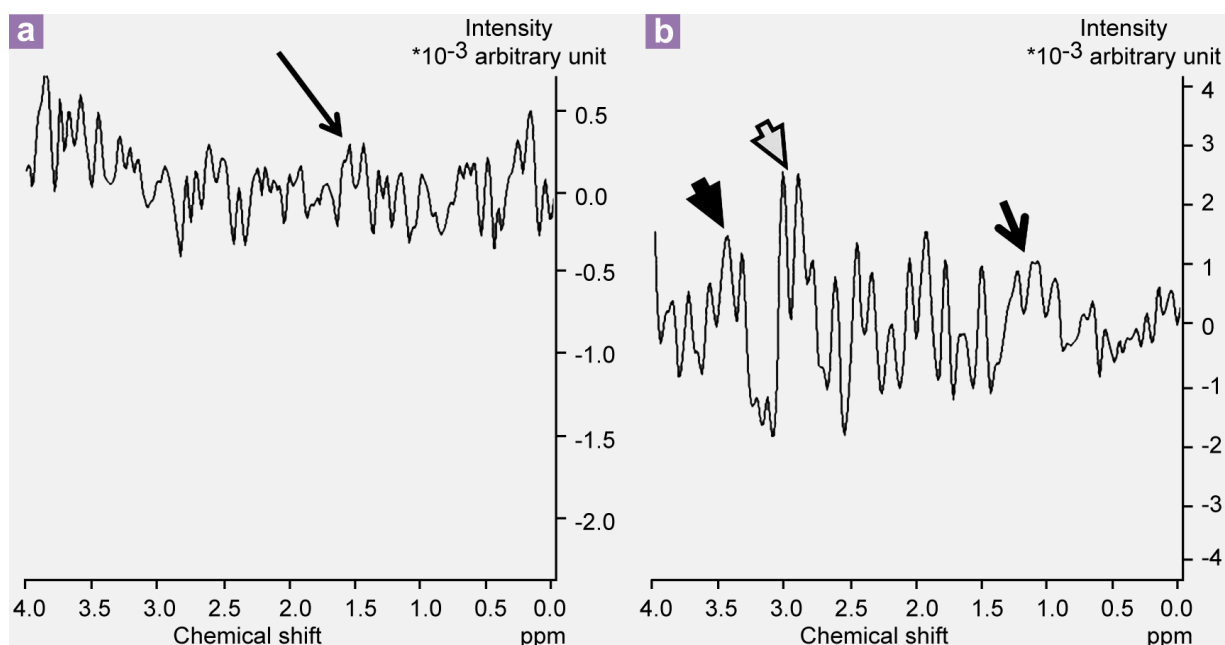


Figure 2: Magnetic resonance (MR) spectroscopy. The MR spectrum shows peaks for the following metabolic products: lactate, lipid, acetate and alanine in the range of 0.9–1.4 ppm (black arrow) in splenic nodules (a), choline-creatine peaks at 3–3.2 ppm (white arrowhead), lipid-lactate peaks at 0.9–1.4 ppm (arrow) and myo-inositol-glycine peaks at 3.6 ppm (black arrowhead) in liver parenchyma (b).

also detected lipid peaks in 15 patients (9). In our study, we observed that major resonance was caused by choline-creatine at 3.2 ppm in the proton MRS of the liver. Moreover, lipid-lactate peaks and myo-inositol-glycine peaks were detected in liver parenchyma. In addition, we observed lipid-lactate peaks and acetate-alanine peaks in the spectroscopy of splenic nodules. In their study, Fischbach et al. detected that major resonance was caused by lipid at 0.8–2.3 ppm and choline at 3.2 ppm on proton MRS of normal livers. The dominant lipid peak belongs to methylene protons at 1.3 ppm. Moreover, the resonances of myo-inositol, glycogen and glucose were detected at 3.35–3.9 ppm. The resonances of threonine, lactate, alanine, glutamine/glutamate, creatine and phosphocreatine cannot be detected in vivo studies owing to their low concentration. However, they have been observed in in vitro studies (10).

Conclusion

MRI is a reliable method in the diagnosis and follow-up of GD thanks to its high-resolution multiplanar imaging capacity. Coupling DW-MRI and MRS with conventional MRI allows for quantitative evaluation, thereby increasing the efficacy of the method. Previously, DW-MRI and MRS findings from the liver and spleen in patients with GD have not been reported in the literature; this is the first report presenting advanced MRI findings from the viscera in GD. The results of DW-MRI and MRS may be much more reliable in large-scale studies. Future investigation is needed to explore the usefulness of these advanced techniques on the evaluation of the abdominal viscera in GD patients.

Acknowledgement

This article presented as 'e-poster' in 30. National Radiology Congress, November 4th–9th 2009, Antalya/Turkey.

Conflict of Interest

The authors of this paper have no conflicts of interest, including specific financial interests, relationships, and/or affiliations relevant to the subject matter or materials included.

Funds

None.

Authors' Contributions

Conception and design, analysis and interpretation of the data, drafting of the article, critical revision of the article for the important intellectual content and final approval of the article: TOK, GE, RK, AK, AA

Provision of study materials or patient: TOK, GE

Correspondence

Dr Ozlem Tugce Kalayci
MD (IKCU), Mmed Rad (IKCU)
Department of Radiology
Izmir Katip Celebi University Atatürk Training and Research Hospital
Gazeteci Hasan Tahsin Caddesi, Yeşilyurt
35160, Izmir, Turkey
Tel: +90-232 2454545 @ +90-530227 0218
Fax: +90-232 2433208
Email: doktorozlemtugce@gmail.com

References

1. Takebayashi S, Iso S, Nagano Y, Kunisaki C, Murakami A, Sasaki T. CT findings of Gaucher disease with large, calcified splenic masses mimicking tumors. *EJR Extra*. 2009;**69**(2):e65–e68. doi: <http://dx.doi.org/10.1016/j.ejrex.2008.07.008>
2. Terk MR, Esplin J, Lee K, Magre G, Colletti P. MR imaging of patients with type I Gaucher's disease: relationship between bone and visceral changes. *AJR Am J Roentgenol*. 1995;**165**(3):599–604.
3. Razek AA, Abdalla A, Fathy A, Megahed A. Apparent diffusion coefficient of the vertebral bone marrow in children with Gaucher's disease type I and III. *Skeletal Radiol*. 2013;**42**(2):283–287. doi: [10.1007/s00256-012-1464-8](https://doi.org/10.1007/s00256-012-1464-8).
4. Razek AA, Abd El-Gaber N, Abdalla A, Fathy A, Azab A, Rahman AA. Apparent diffusion coefficient value of the brain in patients with Gaucher's disease type II and type III. *Neuroradiology*. 2009;**51**(11):773–779. doi: [10.1007/s00234-009-0548-1](https://doi.org/10.1007/s00234-009-0548-1).
5. Hill SC, Damaska BM, Ling A, Patterson K, Di Bisceglie AM, Brady RO, et al. Gaucher disease: abdominal MR imaging findings in 46 patients. *Radiology*. 1992;**184**(2):561–566.
6. Poll LW, Koch JA, vom Dahl S, Sarbia M, Häussinger D, Mödder U. Gaucher disease of the spleen: CT and MR findings. *Abdom Imaging*. 2000;**25**(3):286–289.
7. Kılıçkesmez Ö, Yirik G, Bayramoğlu S, Cimilli T, Aydın S. Non-breath-hold high b-value diffusion-weighted MRI with parallel imaging technique: apparent diffusion coefficient determination in normal abdominal organs. *Diagn Interv Radiol*. 2008;**14**(2): 83–87.

8. Koh DM, Collins DJ. Diffusion-weighted MRI in the body: applications and challenges in oncology. *AJR Am J Roentgenol*. 2007;**188(6)**:1622–1635.
9. Razeq AA, Abdalla A, Gaber NA, Fathy A, Megahed A, Barakat T, Latif Alsayed MA. Proton MR Spectroscopy of the brain in children with neuronopathic Gaucher's disease. *Eur Radiol*. 2013;**23(11)**:3005–3011. doi: 10.1007/s00330-013-2924-9.
10. Fischbach F, Schirmer T, Thormann M, Freund T, Rieke J, Bruhn H. Quantitative proton magnetic resonance spectroscopy of the normal liver and malignant hepatic lesions at 3.0 Tesla. *Eur Radiol*. 2008;**18(11)**:2549–2558. doi: 10.1007/s00330-008-1040-8.